Title

Fluorescent biosensor imaging meets deterministic mathematical modelling: quantitative investigation of signalling compartmentalization.

Journal

The Journal of Physiology, 601(19)

Authors

Posner, Clara

Mehta, Sohum

Zhang, Jin

Publication Date

2023-10-01

DOI

10.1113/JP282696

Peer reviewed

HHS Public Access

Author manuscript

J Physiol. Author manuscript; available in PMC 2024 October 01.

Published in final edited form as:

J Physiol. 2023 October ; 601(19): 4227–4241. doi:10.1113/JP282696.

Fluorescent Biosensor Imaging Meets Deterministic Mathematical Modeling: Quantitative Investigation of Signaling Compartmentalization

Clara Posner[1,2], **Sohum Mehta**[1], **Jin Zhang**[1,2,3,$]

[1]Department of Pharmacology, University of California, San Diego, La Jolla, CA 92093, USA

[2]Shu Chien-Gene Lay Department of Bioengineering, University of California, San Diego, La Jolla, CA 92093, USA

[3]Department of Chemistry and Biochemistry, University of California, San Diego, La Jolla, CA 92093, USA

Abstract

Cells execute specific responses to diverse environmental cues by encoding information in distinctly compartmentalized biochemical signaling reactions. Genetically encoded fluorescent biosensors enable the spatial and temporal monitoring of signaling events in live cells. Temporal and spatiotemporal computational models can be used to interpret biosensor experiments in complex biochemical networks and to explore hypotheses that are difficult to test experimentally. In this review, we first provide brief discussions of the experimental toolkit of fluorescent biosensors as well as computational basics with a focus on temporal and spatiotemporal deterministic models. We then describe how we used this combined approach to identify and investigate a protein kinase A (PKA) – 3′,5′-cyclic adenosine monophosphate (cAMP) – Ca^{2+} oscillatory circuit in MIN6 β cells, a mouse pancreatic β cell system. We describe the application of this combined approach to interrogate how this oscillatory circuit is differentially regulated in a nano-compartment formed at the plasma membrane by the scaffolding protein A-Kinase Anchoring Protein 79/150 (AKAP79/150). We leveraged both temporal and spatiotemporal deterministic models to identify the key regulators of this oscillatory circuit, which we confirmed with further experiments. The powerful approach of combining live-cell biosensor imaging with quantitative modeling, as discussed here, should find widespread use in the investigation of spatiotemporal regulation of cell signaling.

Abstract Figure Description.

Complex cross-regulation between cAMP, PKA, and calcium in β cells leads to coordinated oscillatory behavior, which can be measured in individual cells using genetically encoded fluorescent biosensors. Furthermore, subcellular targeting of genetically encoded fluorescent

[$]To whom correspondence and material requests should be addressed.

Author Contributions

All authors have approved the final version of the manuscript and agree to be accountable for all aspects of the work. All persons designated as authors qualify for authorship, and all those who qualify for authorship are listed.

Competing Interests

The authors declare no conflict of interest.

biosensors enables the detection of compartment-specific, coordinated oscillations of signaling components in cells. The underlying mechanisms behind the coordinated oscillations can be investigated using temporal (ODE) and spatiotemporal (PDE) computational models. This figure was made using Biorender.com.

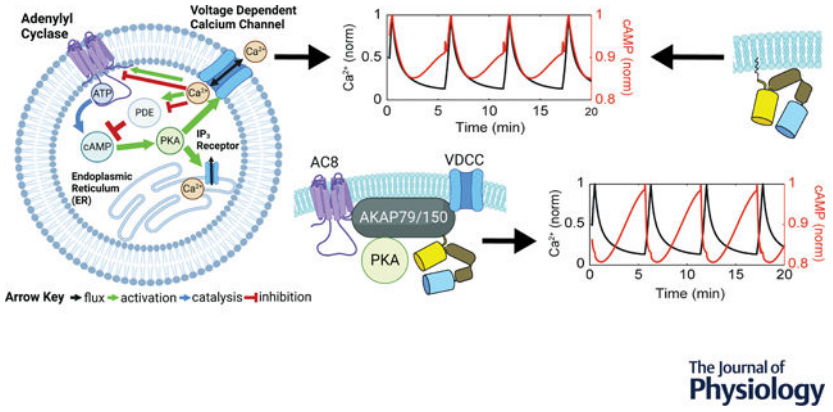

Compartmentalized Signaling

Cell signaling is spatially compartmentalized to coordinate specific and diverse cellular responses to environmental cues. Mechanisms of spatial compartmentalization include intrinsic membrane compartments, molecular assemblies, and dynamic regulatory fencing. Membranes divide eukaryotic cells into intrinsic compartments, such as the plasma membrane, the nucleus, the endoplasmic reticulum, the Golgi apparatus, vesicles, and lysosomes, which each can contain distinct signaling environments. Alternative to membrane partitioning, proteins and other signaling molecules can assemble into molecular assemblies. Multivalent scaffolding proteins can form molecular assemblies by tethering together different proteins and anchoring the assembly to different subcellular locations. Molecular assemblies can also form by liquid-liquid phase separation (LLPS), in which certain biomolecules separate from the general intracellular environment and become enriched in distinct liquid-like droplets called biomolecular condensates or membraneless organelles. Finally, within the context of reaction-diffusion systems, competing regulatory enzymes can impose dynamic spatial boundaries on diffusible signals, a phenomenon we call dynamic regulatory fencing, which often yields spatial signaling gradients. For a more extensive discussion of compartmentalized signaling, please refer to our other reviews (Mehta and Zhang 2021; J. F. Zhang et al. 2021).

Genetically Encoded Fluorescent Biosensors

Genetically encoded fluorescent biosensors are protein-based probes that convert a biochemical signaling event into a change in the sensor’s fluorescent properties, which can then be measured optically. These biosensors are particularly useful for investigating compartmentalized signaling, as they can be targeted to different subcellular compartments. Biosensors have been developed to detect the presence of intracellular messengers, metabolites, and other analytes, or track changes in the localization, conformation, and activity of signaling proteins. Biosensors typically consist of two functional regions—a

sensing unit and a reporting unit. The sensing unit can either bind directly to the target of interest or be chemically modified by the target, which induces a change in the reporting unit. Sensors can be broadly categorized by two different reporting mechanisms: reporting by changes in cellular location or changes in fluorescence signal (please see E. C. Greenwald et al. 2018 for a more comprehensive review of genetically encoded biosensors).

Genetically encoded sensors that report by changes in cellular location generally consist of a fluorescent protein (FP) fused to a sensing protein that can bind to the target molecule of interest. When the reporter translocates and binds to the target molecule, the resulting redistribution of fluorescence to a particular location indicates the local generation of the target molecule. One example of this reporter design involves tethering the binding-domain of an endogenous effector protein to an FP. This design has been used to sense membrane lipids (Várnai et al. 1999) as well as GTP-loaded Ras and Rap GTPases (Bivona and Philips 2005). Alternative to endogenous effector proteins, “nanobodies” or heavy chain-only antibodies that bind to the target of interest, or even a specific conformation of a target protein, can also be tagged with an FP to visualize endogenous target proteins (de Beer and Giepmans 2020). For example, a GFP-labeled nanobody that selectively binds to agonist-bound and thus activated β_2-adrenoceptor has been used to visualize the internalization and trafficking of activated receptor in live cells (Irannejad et al. 2013). Kinase translocation reporters (KTRs) represent another type of location-based reporters that translocate to a particular subcellular region in response to a stimulus (Kudo et al. 2018). The KTR sensing domain consists of a kinase substrate motif fused to a bipartite nuclear localization signal (bNLS) and a nuclear export signal (NES). When the KTR is phosphorylated by the kinase of interest, the negatively charged phosphate groups will decrease bNLS function, causing the KTR to translocate out of the nucleus and into the cytoplasm. KTRs have been developed for several different kinases, including Extracellular-Signal Regulated Kinase (ERK), c-Jun N-terminal Kinase (JNK), p38 kinases, and Protein Kinase A (PKA) (Regot et al. 2014).

In addition to translocation-based sensors, biosensors can report detection of the target molecule via a change in fluorescence. Typically, the target can either post-translationally modify or simply bind to the sensing unit, causing a conformational change that alters the fluorescence output of the reporting unit. A sensing unit that undergoes a conformational change in response to a stimulus is also referred to as a molecular switch. This design can be implemented by incorporating a molecular switch directly into the β-can of a single FP (Nasu et al. 2021). When the molecular switch interacts with the target molecule, it undergoes a conformational change that alters the FP structure, which in turn changes the fluorophore properties, such as increasing or decreasing the fluorescence intensity or shifting the peak excitation or emission wavelength. This single-fluorophore design has been used in genetically encoded calcium indicators (GECIs) and in biosensors for membrane potential, cAMP and cGMP, and kinase activities (E. C. Greenwald et al. 2018).

Another implementation consists of a molecular switch sandwiched between two fluorescent proteins capable of Förster resonance energy transfer (FRET), a radiationless energy transfer via dipole coupling from a donor fluorophore to an acceptor fluorophore (J. F. Zhang et al. 2021). This energy transfer causes a decrease in donor fluorescence and a corresponding

increase in acceptor fluorescence upon donor excitation, which can be reported as the ratio of acceptor to donor emission intensity or detected as a donor fluorescence lifetime change. This FRET-based design has been used in biosensors for metal ions, intracellular messengers, phosphoinositides and kinase activities (J. F. Zhang et al. 2021). For FRET-based kinase activity reporters, the molecular switch contains a kinase substrate motif connected to a phosphoamino-acid binding domain by a flexible linker. When the kinase of interest phosphorylates the substrate motif on the biosensor, the phosphoamino-acid binds to phosphorylated substrate motif, causing a conformational change in the sensor that modulates the FRET readout.

Each biosensor design approach has pros and cons that should be weighed carefully before experiments are conducted. When measuring small changes in signaling activities, it is best to select a biosensor with the highest sensitivity, i.e., high signal-to-noise ratio and high affinity for the target (Palmer et al. 2011). However, sometimes the highest-affinity sequences may suffer from reduced selectivity and can sense other molecules than the desired target (Palmer et al. 2011). When investigating differences in kinase activity in different subcellular compartments, KTRs would be less desirable as they use translocation as a readout of kinase activity and thus cannot be readily used to probe the activity in different compartments. If the research question involves probing the interplay between multiple signaling molecules, intensiometric single-FP sensors would be attractive since they occupy less spectral space and can be used in multiplexed imaging of many different, spectrally orthogonal biosensors. However, variability in protein expression and illumination intensity can affect fluorescence intensity independent of target activity, making it difficult to quantitatively measure signaling activities (Germond et al. 2016).

Finally, when detecting compartmentalized signaling activities, one must also consider the potential effects of subcellular compartments on biosensor reporting. When targeted to acidic environments such as endosomes and lysosomes, biosensors should employ specific fluorescent proteins that are insensitive to acidic pH (Betolngar et al. 2015; Burgstaller et al. 2019). When targeted to oxidative environments in the secretory pathway, such as the endoplasmic reticulum and Golgi, biosensors should use fluorescent proteins that are resistant to forming disulfide bonds that may cause misfolding of the fluorescent protein (Costantini et al. 2015).

Computational Modeling

Due to the complexity of spatiotemporal signaling networks, mathematical modeling can aid in investigating network compositions and mechanisms that are too complex to infer from biosensor imaging data alone. Mathematical models can also be applied to test conditions that are difficult to achieve experimentally. Modeling based on experimental data is an iterative process, starting with a hypothesized network topology (or multiple topologies). A model is built with reactions based on this hypothesized network and then applied to generate predictions (J. H. Yang and Saucerman 2011). Next, model predictions are compared against experimental results, and if they do not match, the model topology requires refinement, initiating the process again. Even models that do not match experimental results provide useful information, as they indicate that processes outside

of those included in the model are important in the observed experimental phenomenon, generating new avenues of investigation.

Two main types of models are deterministic models, which are differential equation-based models and will yield the same results for a set of given initial conditions, or stochastic models, which incorporate randomness or uncertainty to represent noise and as a result, yield different results for each simulation. Stochastic models are better suited for low protein numbers, low volumes, and noisy systems. For this review, we focus on deterministic models, and readers are referred to other reviews for more information on stochastic modeling (Gonze et al. 2018; Székely and Burrage 2014; Tyson et al. 2019). In deterministic models, one can examine the biochemical activity in cells by using ordinary differential equation (ODE)-based models, in which the concentration or number of molecules varies only in time, or by using partial differential equation (PDE)-based models, in which the concentration or number of molecules varies in both time and space. As PDE models contain more independent variables than ODE models, they are typically more complex and more difficult to solve.

There are some alternative models for representing complex biological signaling processes. In particular, rule-based or agent-based models treat individual signaling molecules as “agents”, and their properties such as biomolecular interactions and diffusion are represented as local rules (Chylek et al. 2014; Soheilypour and Mofrad 2018). Bayesian network models represent probabilistic dependence between signaling network components, which may imply a functional connection between them (Sachs et al. 2005). Since Bayesian models are probabilistic, they are more robust to noisy biological data, and they are useful for identifying the most probable network topologies from a collection of hypothesized signaling networks (Sachs et al. 2002, 2005).

Temporal Kinetic Models using Ordinary Differential Equations (ODEs)

Temporal ODE-based models answer questions about how the concentration of a component of interest changes in time in a well-mixed compartment. ODE models are useful in mechanistically investigating complex temporal activity and regulation in large biochemical systems containing many signaling components and reactions. For example, Zhang et al. created an ODE model to investigate the mechanism behind the biphasic RhoA response to histamine stimulation observed using a FRET-based RhoA activity sensor and found that the first phase of biphasic RhoA activation depended on both p63 Rho Guanine Nucleotide Exchange Factor (RhoGEF) and continuously active histamine receptor, while the second phase depended on p115 RhoGEF, independent of histamine receptor activity (J. Z. Zhang, Nguyen, et al. 2020).

In another example, Ryu et al. measured the kinetics of growth factor-stimulated Extracellular Signal-Regulated Kinase (ERK) activity in single cells using a FRET-based ERK biosensor and observed a heterogeneous mix of transient and sustained ERK kinetics across different cells in response to sustained growth factor stimulation (Ryu et al. 2015). On the other hand, when they applied pulsed growth factor stimulation instead of sustained stimulation, they observed homogeneous ERK transients across a population of cells. To investigate the mechanism behind the heterogenous responses across different cells, they

built a semi-deterministic ODE model, in which individual cells were simulated by assigning initial signaling component concentrations taken randomly from a log-normal distribution corresponding to the distribution of protein abundances across the cell population. From this model, they identified that a receptor activity-dependent, feed-forward mechanism from ERK on an upstream kinase in the signaling cascade is responsible for the heterogenous ERK kinetics and that this mechanism is bypassed during pulsed growth factor stimulation.

ODEs assume that concentrations are uniform throughout the volume, which may differ greatly from physiological conditions. Compartmental ODE models can therefore be implemented to account for differing signaling activities and concentrations in different subcellular locations. While compartmental ODE models still assume the components within each compartment are well mixed, they can offer some insight into differences in signaling activities between different spatial compartments while maintaining simplicity compared to PDE models. Compartmental ODE models can be used to probe signaling behaviors in multiple subcellular compartments, such as different organelles or even microdomains within the same organelle.

For example, Yang et al. implemented a compartmental ODE model to investigate the mechanism behind kinetic and sensitivity differences in β-adrenergic receptor agonist-stimulated PKA activity in the nucleus compared to the cytosol in cardiomyocytes, which they observed using a FRET-based PKA activity biosensor. Their model predicted that the slower and weaker PKA activity in the nucleus is due to the slow diffusion of PKA catalytic subunit into the nucleus and that the sensitivity differences are regulated by nuclear expression of protein kinase inhibitor (PKI) (J. H. Yang et al. 2014). In experiments using a nuclear-targeted PKA activity biosensor, they measured a further decrease in nuclear PKA activity when nuclear transport was inhibited, confirming that slow diffusion of PKA catalytic subunit into the nucleus rate-limits nuclear PKA activity. They also confirmed via immunostaining that PKI was localized exclusively to the nucleus in the cardiomyocytes.

In another example, using both biosensor experiments and a compartmental ODE model, Agarwal et al. investigated whether cAMP production differs at the plasma membrane in lipid rafts, a plasma membrane microdomain enriched in cholesterol, versus in non-raft domains, since cAMP-stimulating receptors and proteins are non-uniformly distributed between these microdomains (Agarwal et al. 2014). Using FRET-based cAMP reporters localized to these different regions, they observed a greater maximal cAMP biosensor response to receptor activation in lipid-raft regions than in non-raft regions of the plasma membrane. Adenyl cyclase inhibition alone caused a decrease in the biosensor response only in the non-raft regions, indicating that this difference in maximal cAMP responses was due to higher basal cAMP in non-raft plasma membrane regions. Through their compartmental ODE model, they found that limited diffusion of cAMP between these microdomains was integral to the observed cAMP compartmentation at the plasma membrane.

Spatiotemporal Kinetic Models using Partial Differential Equations (PDEs)

While compartmental ODE models can be used to investigate signaling activity within different compartments, to investigate the effect of spatial concentration gradients and cell morphology on signaling dynamics, one needs to implement PDE-based models, as these

explicitly measure changes in the concentration or number of molecules in space as well as time. While PDEs can include variables for all three spatial dimensions, simplifying to only one to two spatial dimensions can reduce computational complexity.

For example, Lohse et al., investigated whether phosphodiesterases can create cAMP nano-compartments by creating a FRET-based cAMP biosensor fused to the phosphodiesterase PDE4A1, which enables the measurement of cAMP concentrations in the immediate vicinity of the enzyme (Lohse et al. 2017). They observed experimentally with this sensor that phosphodiesterase activity can create a local cAMP sink. However, their computational PDE-based model of cAMP concentration with respect to time and radial distance from the sensor predicted that phosphodiesterase activity alone cannot generate the experimentally observed cAMP compartmentation.

In another example, Takano et al. investigated whether RhoA and Rho-kinase contribute to the formation of a single axon from many minor neurites in polarized neurons (Takano et al. 2017). Using photoactivatable RhoA and Rho-kinase, they found that polarized activation of RhoA and Rho-kinase is sufficient to cause minor neurites to retract. They built a PDE-based model of Rho-kinase diffusion along minor and long neurites, which predicted greater accumulation of Rho-kinase in minor neurites compared to the long neurite. They validated this prediction experimentally using immunostaining.

Considerations for Constraining Computational Models with Biosensor Data

When fitting computational models to biosensor data, one must first determine how to quantitatively relate the changes in biosensor fluorescence signal to the signaling activity being measured. Depending on the biosensor target and the existence of pathway activators and inhibitors, calibration can be performed in cells or using purified sensors in vitro. Ideally, calibration performed using techniques as close to the physiological conditions as possible will yield the most accurate results.

One calibration approach is to normalize the experimentally measured biosensor signal to minimum and maximum activation in cells. This normalization requires being able to experimentally obtain the minimal activity from low basal activity, inhibitors, or negative-control mutant sensors and maximal activity from activators, as well as inhibition of signal degraders, to calculate the fraction of total biosensors that are active (E. Greenwald et al. 2014; Regot et al. 2014). Sensors for membrane-impermeable analytes or pH can be calibrated in cells using chemicals that permeabilize the membrane to the analyte so that its intracellular concentration equilibrates with the applied extracellular concentration (Arosio et al. 2010; Chin et al. 2021). When maximal stimulation is not experimentally feasible for sensors that detect post-translational modifications or GTP loading, calibration can be performed by immunoblotting of activated sensor and total sensor (Fujioka et al. 2006; Gillies et al. 2020). For smaller molecules or ions that cannot be detected by immunoblotting, biosensors can also be purified and calibrated with known concentrations of analyte in vitro. However, calibration of the sensors in vitro assumes that the maximal sensor response is similar in vitro and in cells, which may not be applicable across various primary cell types (Börner et al. 2011).

The next consideration is whether to explicitly incorporate the biosensor and its activating reactions into the computational model or to relate the fluorescence signal to the active species in the model. If the model is constrained such that the range of signaling activities are within the detection limits of the biosensors, i.e., the biosensors do not become saturated, the biosensor signal can be directly related to the parameters of activated species in the model (Fujita et al. 2014; J. Z. Zhang, Nguyen, et al. 2020). However, if the sensor kinetics differ from the signaling event being detected, such as delayed onset kinetics or delayed signal decay kinetics, this modeling approach might not yield accurate predictions. In such a case, a correction factor that relates biosensor kinetics to actual signaling kinetics could be calculated to compensate for such discrepancies (Lai et al. 2007).

A final consideration is that genetically encoded biosensors may perturb endogenous signaling activities. For example, when biosensors bind their targets, they can sequester the analyte and thus decrease the overall cell concentration, a phenomenon known as buffering (E. Greenwald et al. 2014). Buffering can be minimized as long as biosensor expression levels are kept low (E. Greenwald et al. 2014). Alternatively, biosensor expression levels can be estimated, and the sensor concentration explicitly included in the model to account for buffering effects (Falkenburger et al. 2010).

Probing Temporal and Compartmental Behavior of a Ca^{2+}-cAMP-PKA Oscillatory Circuit in MIN6 Cells

Temporal phase regulation of a Ca^{2+}-cAMP-PKA oscillatory circuit

In our previous work, we combined biosensor experiments with computational modeling to investigate complex cross-regulation of cAMP/PKA and Ca^{2+} signaling in MIN6 cells, a mouse pancreatic β-cell line (Ni et al. 2011). Cytosolic Ca^{2+} oscillations trigger pulsatile insulin secretion in pancreatic β-cells, which is an important function that is dysregulated in type 2 diabetes (MacDonald and Rorsman 2006). Ca^{2+} oscillations depend on Ca^{2+} influx across the plasma membrane, which is regulated by voltage-dependent Ca^{2+} channels (VDCCs), and Ca^{2+} release from internal stores in the endoplasmic reticulum, which is controlled by inositol triphosphate receptors (IP_3Rs). PKA can modulate Ca^{2+} signaling by phosphorylating and activating both VDCCs (Ammala et al. 1993) and IP_3Rs (Desouza et al. 2002). Ca^{2+} and its downstream effectors can also modulate cAMP levels and PKA, which is activated by cAMP, by activating or inhibiting adenyl cyclases (ACs) and phosphodiesterases, which catalyze the production and degradation of cAMP, respectively (Seino and Shibasaki 2005). Our study focused on specifically measuring the dynamics of PKA activity in this system and investigating the role of PKA dynamics on this complex feedback system with Ca^{2+} (Figure 1A).

While kinases are typically thought of as on-off switches, when we visualized PKA activity with a FRET-based A kinase activity reporter (AKAR) in MIN6 cells treated with tetraethylammonium (TEA), an agent that depolarizes the plasma membrane to trigger Ca^{2+} influx, we observed oscillations in PKA activity. Fluorescent biosensor imaging enabled the detection of these oscillations that population-based methods such as immunoblotting could not resolve due to asynchronous oscillations among individual cells. We then investigated

the correlation between Ca^{2+} and PKA activity oscillations by multiplexing the Ca^{2+} dye Fura-2 with AKAR or the FRET-based cAMP sensor Indicator of cAMP using Epac (ICUE) and found synchronized oscillations between all three signaling activities (Figure 1B - D). We observed that Ca^{2+} oscillations are antiphase with cAMP oscillations (Figure 1D) and that the Ca^{2+} peak onset lags behind PKA activity peak onset (Figure 1C), hinting at PKA-mediated activation of VDCCs and/or IP_3Rs. We also observed that PKA activity decay was correlated with the onset of Ca^{2+} spikes, suggesting cAMP/PKA regulation by Ca^{2+}-dependent ACs or PDEs.

To investigate the mechanism of interplay between Ca^{2+}, cAMP and PKA, we built a minimal ODE model that was sufficient to recapitulate the experimental findings (Figure 1E and F). We first performed topology analysis and determined that the inclusion of Ca^{2+}-bound calmodulin (CaM)-mediated activation of PDEs was sufficient to computationally reproduce the experimentally observed antiphase Ca^{2+} and cAMP oscillations. The final model used reactions and parameters from previously published models, but we tuned parameters affecting Ca^{2+} oscillation frequency such that the model predicted Ca^{2+} oscillations that matched this experimental system, as previous values were derived from other cell lines with different Ca^{2+} oscillation frequencies. We also explicitly included Fura-2, ICUE, and AKAR in the model, with their reaction parameters estimated from previous studies, to enable direct comparison between model predictions and experimental results. The combined experimental and modeling data led to the discovery of an oscillatory circuit consisting of Ca^{2+}, cAMP and PKA.

We used this model to evaluate the role of PKA in this oscillatory system. Inhibiting PKA in the model abolishes Ca^{2+} oscillations (Figure 2A), while activating PKA increases oscillation frequency (Figure 2B). We confirmed this experimentally by adding H89, an ATP-competitive PKA inhibitor, (Figure 2C) or 3-isobutyl-1-methylxanthine (IBMX), a phosphodiesterase inhibitor that indirectly activates PKA by increasing cAMP levels (Figure 2D). Furthermore, model sensitivity analysis identified that the frequency, but not amplitude, of Ca^{2+} oscillations was sensitive to PKA activity, indicating that PKA acts as a Ca^{2+} frequency modulator in this circuit.

We next asked whether direct activation of PKA can trigger the oscillations of this signaling system. We found that sufficiently strong PKA feedback can tune as well as initiate oscillations even when the model branch involving Ca^{2+} and membrane potential is initially inactive (Figure 2E). To experimentally verify this prediction, we applied a low dose (1–3 μM) of 8-bromoadenosine-3′, 5′-cyclic monophosphate acetoxymethylester (8-Br-cAMP-AM), a cell-permeable cAMP analog that preferentially activates PKA, to cells expressing AKAR and found that this low PKA input signal triggered oscillatory changes in PKA activity (Figure 2F). Higher doses (10–20 μM) of 8-Br-cAMP-AM induced a different PKA behavior – smaller amplitude and higher frequency oscillations superimposed on a monotonic activity increase (Figure 2F). Our model predictions qualitatively matched these results (Figure 2E).

We then investigated the functional consequences of these varying PKA oscillations under low and high stimulation conditions. We found that low doses of the cAMP analog induced

oscillations in the cytosol without affecting nuclear PKA activity, which we determined by measuring PKA phosphorylation of a nuclear substrate, the endogenous transcription factor CREB. High doses of the analog, on the other hand, caused a gradual increase in PKA activity with superimposed high-frequency oscillations and led to an increase in nuclear PKA activity and CREB phosphorylation.

Our results suggest that oscillatory PKA activity enabled by the Ca^{2+}-cAMP-PKA circuit can serve as a distinct mechanism for achieving signaling diversity. The frequency of PKA activity oscillation can encode specific signaling information, based on the identities and doses of input signals, and generate specific functional output – depending on the frequency of oscillations, the system may switch from a local (cytosol only) to a global (cytosol plus nucleus) signaling mode. Furthermore, we discovered that PKA also controls the oscillatory patterns of other key components in the signaling circuit, such as Ca^{2+}. Our findings indicate that complex cell functions may depend on the coordination and synchronization of multiple oscillating signaling components.

While the model in this study was sufficient to qualitatively reproduce the Ca^{2+}-cAMP-PKA oscillations, discrepancies between the predicted PKA and Ca^{2+} oscillation behavior (Figure 1E) and the experimental observations (Figure 1C) are apparent, highlighting the potential for further refinement of the model. The discrepancy is likely because we evaluated the possible minimal model topologies using two criteria that only relate cAMP and Ca^{2+} oscillations. Re-evaluating these hypothesized topologies with a 3rd criterion that the Ca^{2+} and PKA oscillations are in-phase may improve performance. Simplifications and assumptions within the model, such as the simplified interactions between the Ca^{2+} and cAMP modules and the assumption that calmodulin modulates adenylyl cyclases and phosphodiesterases in the same manner, may also need to be adjusted to satisfy this 3rd criterion. This improved model would aid in further investigation into the mechanism of PKA regulation of Ca^{2+} oscillations.

Spatially compartmentalized phase regulation of the Ca^{2+}-cAMP-PKA oscillatory circuit

Considering that cAMP and Ca^{2+} are differentially regulated at different spatial compartments, we expanded on our previous discovery of the Ca^{2+}-cAMP-PKA oscillatory circuit to investigate how this circuit is regulated at a distinct plasma membrane localized nano-compartment formed by the scaffolding protein AKAP79/150. AKAP79/150 has been previously demonstrated to be important in this pathway, as knocking-out AKAP79/150 functionally impaired glucose-stimulated insulin secretion in β-cells (Hinke et al. 2012). Since AKAP79/150 tethers a unique combination of key oscillatory circuit components, i.e. VDCC, adenylyl cyclase 8 (AC8), and PKA (Tenner et al. 2020), we hypothesized that the AKAP79/150 scaffold creates a compartment with fine-tuned Ca^{2+}-cAMP-PKA oscillatory circuit dynamics.

We first experimentally investigated this hypothesis by targeting a FRET-based cAMP biosensor (Epac1-camps) to either the AKAP79/150 compartment or the general plasma membrane and performed multiplexed imaging along with a red-fluorescent Ca^{2+} biosensor (RCaMP) (Figure 3A and B). We observed at the general plasma membrane that cAMP oscillations were out-of-phase with Ca^{2+} oscillations (Figure 3A), consistent with the

behavior observed in the cytoplasm in our previous study, but at the AKAP79 compartment, cAMP was found to oscillate in-phase with Ca^{2+} oscillations (Figure 3B).

To gain a more quantitative understanding of the regulation of the cAMP-Ca^{2+} phase relationship at the AKAP79 compartment, we created a simplified well-mixed model based on our previous model to investigate the role of ACs and phosphodiesterases. This simplified model contained reactions for Ca^{2+}, cAMP, Ca^{2+}-stimulated AC8 and the phosphodiesterase PDE1 (Figure 3C). The model predicted that the phase relationship between cAMP and Ca^{2+} can be tuned by altering the relative strength between ACs and phosphodiesterases. When AC8 dominates, cAMP and Ca^{2+} oscillate in phase; conversely, when PDE1 dominates, oscillations are out of phase. We experimentally confirmed this prediction by knocking down AC8, which caused the previously in-phase cAMP-Ca^{2+} oscillations in the AKAP79/150 compartment to shift out of phase. Conversely, when we increased AC8 levels at the plasma membrane by overexpressing AC8, cAMP oscillations outside the AKAP79/150 compartment shifted in phase with Ca^{2+} oscillations.

cAMP must be distinctly regulated within the AKAP79/150 nano-compartment and the general plasma membrane compartment to produce the observed differences in cAMP oscillations within these proximal compartments. The mechanisms that regulate cAMP compartmentation, however, are not completely understood, especially considering that single cAMP-producing ACs and cAMP-degrading phosphodiesterase enzymes have relatively low catalytic efficiency (Bock et al. 2020; Conti et al. 2014; J. Z. Zhang, Lu, et al. 2020). Previously, we found that AKAP79/150 forms nanometer-scale clusters along the plasma membrane (Mo et al. 2017). Because AKAP79/150 and AC8 are known to interact (Willoughby et al. 2012), we hypothesized that AC8 may similarly form plasma membrane nanoclusters to compartmentalize cAMP production. We tested this hypothesis by performing super-resolution imaging of AKAP79/150 and AC8 and found that AKAP79/150 forms clusters, as previously observed (Mo et al. 2017), and that AC8 also forms clusters as well. We calculated the mean radius and average nearest neighbor spacing for both molecules and performed Fluorescence Recovery after Photobleaching (FRAP) to measure the diffusivity of AC8.

We then used these data to build a spatial model using the simplified model reactions to test whether the nano-scale organization of AKAP79/150 and AC8 is important for mediating in-phase oscillations. We created a hexagonal prism with one immobile AKAP79/150:AC8 cluster in the center of the plasma membrane face and PDE1 well mixed throughout the volume to represent cytosolic PDE1 (Figure 3D). The spatial model successfully recapitulated the experimentally observed in-phase Ca^{2+} and cAMP oscillations at the center of the AKAP79/150:AC8 cluster and out-of-phase oscillations at the general plasma membrane or in the cytosol (Figure 3E).

Further, assuming AC8 clustering was driven by AKAP79/150 clustering and AKAP79/150:AC8 interactions, the model predicted that decreasing AC8:AKAP79/150 interactions would lead to a decrease in local AC8 concentration in the nanoclusters (Figure 4A) and a reduction of the spatial domain of in-phase oscillations (Figure 4B). We experimentally verified this prediction by overexpressing the N-terminal 106 residues

of AC8 ($AC8^{1-106}$), which competes with full-length AC8 and disrupts the interaction with AKAP79/150. We found that overexpressing $AC8^{1-106}$ caused a decrease in the number of AC8 molecules within AC8 nanoclusters, as measured via super-resolution microscopy (Figure 4C), and an increase in the number of cells with out-of-phase cAMP oscillations at the AKAP79/150 compartment measured via cAMP imaging (Figure 4D).

We then applied this spatial model to explore the functional role of spatially compartmentalized cAMP-Ca^{2+} phase regulation. Our model predicted that cAMP oscillations also cause PKA oscillations, which we experimentally confirmed by multiplexing AKAR and RCaMP. Furthermore, perturbing the precise nano-compartment phase relationship by inhibiting AC8:AKAP interactions using $AC8^{1-106}$ disrupted the strength and timing of Ca^{2+} oscillations, likely due to defective PKA regulation of VDCCs (e.g., $Ca_V1.2$). These data indicate that the compartmentalization of cAMP- Ca^{2+} oscillatory phase regulates global Ca^{2+} oscillation frequency, regularity, and sustainability.

In this work, we demonstrated the phase relationship between two key components in an oscillatory signaling circuit can be spatiotemporally regulated, representing a novel mode of information encoding. We further show that disruption of the nano-scale compartment regulation impacts global Ca^{2+} oscillations, demonstrating the functional importance of maintaining this organization. The in-phase cAMP and Ca^{2+} oscillations at the AKAP79/150 compartment may play an important role in insulin secretion in β cells, as AKAP79/150 associates with insulin secretory granules via $Ca_V1.2$ (Murphy et al. 2014). This form of information encoding may be a strategy employed by other compartmentalized signaling networks to enable diverse cell signaling responses to stimuli.

Conclusion and Future Perspectives

Combining computational models with fluorescent biosensor imaging enables the quantitative and mechanistic investigation of complex signaling phenomena. Even models that are not able to reproduce key experimental results provide some value, as they indicate the importance of other signaling molecules not defined in the model. Fluorescent biosensor imaging provides both spatial and temporal readouts on the seconds to minutes time scale that are useful for both constructing models and validating model predictions, particularly for models that account for compartmentalized or spatial signaling. Further, fluorescent biosensors can be multiplexed in single cells, which enables the visualization and analysis of correlations between dynamics of multiple signaling components that would be obscured from population-level measurements.

New experimental techniques enable enhanced throughput for quantitative, single-cell dynamic measurements (E. Greenwald et al. 2023) as well as investigations of many different signaling components simultaneously, such as improvements in biosensor multiplexing strategies in single cells (Mehta et al. 2018) or biosensor barcoding schemes in populations of cells (J. M. Yang et al. 2021). With increased information, computational models can serve as a quantitative framework to integrate datasets and enable investigation of complex network behaviors. Studies combining these two approaches will further enable a systems approach to elucidating large and complex spatiotemporal crosstalk mechanisms.

For example, Yang et al. demonstrated the ability to infer feedback loops of various networking components in their biosensor barcoding approach by inhibiting one signaling component at a time and measuring the effects on all other biosensor signals (J. M. Yang et al. 2021). Their approach assumes that the responses of the mixed population of differentially barcoded cells are synchronized to a shared stimulation and environment, but this approach would fail to capture complex signaling behavior such as asynchronous oscillations. In such a case, multiplexing the same sensors in single cells would be a better alternative, but fewer signaling activities can be simultaneously detected compared to the barcoding approach. In either case, the data indicate positive or negative cross-regulation between signaling components but do not illuminate the mechanism. A computational model could be used to investigate possible mechanisms underlying experimentally observed cross-regulation. This would entail building computational models containing hypothesized crosstalk reactions and evaluating which reactions are sufficient for the model to reproduce the experimental results from multiplexed or barcoded biosensor imaging.

Supplementary Material

Refer to Web version on PubMed Central for supplementary material.

Acknowledgements

We thank E.C. Greenwald for critical reading of this manuscript.

Funding

This research was supported by NIH 1F31 CA257381-01A1 to CP and R35 CA197622, R01 DK073368, R01 DE030497, R01 HL 162302, R01 CA262815, RF1 MH123212 and a grant from the Fibrolamellar Cancer Foundation (FCF) to J.Z.

Biography

Clara Posner completed her BS in Bioengineering (2016) at University of California Los Angeles and is completing her PhD in Bioengineering at the University of California San Diego under the supervision of Dr. Jin Zhang. Her research has been supported by the NIH T32 fellowship and the NIH National Cancer Institute F31 fellowship. Her PhD thesis focuses on multiplexing biosensors and applying a liquid handling combined microscope to enhance biosensor imaging throughput.

References

Agarwal SR, Yang PC, Rice M, Singer CA, Nikolaev VO, Lohse MJ, et al. (2014). Role of membrane microdomains in compartmentation of cAMP signaling. PLoS ONE, 9(4), e95835. 10.1371/journal.pone.0095835

Ammala C, Ashcroft FM, Rorsmant P, & Kb B. (1993). Calcium-independent potentiation of insulin release by cyclic AMP in single Beta -cells. Letters to Nature, 363(May), 356–358.

Arosio D, Ricci F, Marchetti L, Gualdani R, Albertazzi L, & Beltram F. (2010). Simultaneous intracellular chloride and pH measurements using a GFP-based sensor. Nature Methods, 7(7), 516–518. 10.1038/nmeth.1471 [PubMed: 20581829]

Betolngar DB, Erard M, Pasquier H, Bousmah Y, Diop-Sy A, Guiot E, et al. (2015). pH sensitivity of FRET reporters based on cyan and yellow fluorescent proteins. Analytical and Bioanalytical Chemistry, 407(14), 4183–4193. 10.1007/s00216-015-8636-z [PubMed: 25814274]

Bivona TG, & Philips MR (2005). Analysis of Ras and Rap activation in living cells using fluorescent Ras binding domains. Methods, 37(2), 138–145. 10.1016/j.ymeth.2005.05.022 [PubMed: 16289969]

Bock A, Annibale P, Konrad C, Hannawacker A, Anton SE, Maiellaro I, et al. (2020). Optical Mapping of cAMP Signaling at the Nanometer Scale. Cell, 182(6), 1519–1530.e17. 10.1016/j.cell.2020.07.035

Börner S, Schwede F, Schlipp A, Berisha F, Calebiro D, Lohse MJ, & Nikolaev VO (2011). FRET measurements of intracellular cAMP concentrations and cAMP analog permeability in intact cells. Nature Protocols, 6(4), 427–438. 10.1038/nprot.2010.198 [PubMed: 21412271]

Burgstaller S, Bischof H, Gensch T, Stryeck S, Gottschalk B, Ramadani-Muja J, et al. (2019). PH-Lemon, a Fluorescent Protein-Based pH Reporter for Acidic Compartments. ACS Sensors, 4(4), 883–891. 10.1021/acssensors.8b01599 [PubMed: 30864782]

Chin MY, Patwardhan AR, Ang KH, Wang AL, Alquezar C, Welch M, et al. (2021). Genetically Encoded, pH-Sensitive mTFP1 Biosensor for Probing Lysosomal pH. ACS Sensors, 6(6), 2168–2180. 10.1021/acssensors.0c02318 [PubMed: 34102054]

Chylek LA, Harris LA, Tung CS, Faeder JR, Lopez CF, & Hlavacek WS (2014). Rule-based modeling: A computational approach for studying biomolecular site dynamics in cell signaling systems. Wiley Interdisciplinary Reviews: Systems Biology and Medicine, 6(1), 13–36. 10.1002/wsbm.1245 [PubMed: 24123887]

Conti M, Mika D, & Richter W. (2014). Cyclic AMP compartments and signaling specificity: Role of cyclic nucleotide phosphodiesterases. Journal of General Physiology, 143(1), 29–38. 10.1085/jgp.201311083 [PubMed: 24378905]

Costantini LM, Baloban M, Markwardt ML, Rizzo M, Guo F, Verkhusha VV, & Snapp EL (2015). A palette of fluorescent proteins optimized for diverse cellular environments. Nature Communications, 6(May). 10.1038/ncomms8670

de Beer MA, & Giepmans BNG (2020). Nanobody-Based Probes for Subcellular Protein Identification and Visualization. Frontiers in Cellular Neuroscience, 14(November), 1–16. 10.3389/fncel.2020.573278 [PubMed: 32038177]

Desouza N, Reiken S, Ondrias K, Yang YM, Matkovich S, & Marks AR (2002). Protein kinase A and two phosphatases are components of the inositol 1,4,5-trisphosphate receptor macromolecular signaling complex. Journal of Biological Chemistry, 277(42), 39397–39400. 10.1074/jbc.M207059200

Falkenburger BH, Jensen JB, & Hille B. (2010). Kinetics of M 1 muscarinic receptor and G protein signaling to phospholipase C in living cells. Journal of General Physiology, 135(2), 81–97. 10.1085/jgp.200910344 [PubMed: 20100890]

Fujioka A, Terai K, Itoh RE, Aoki K, Nakamura T, Kuroda S, et al. (2006). Dynamics of the Ras/ERK MAPK cascade as monitored by fluorescent probes. Journal of Biological Chemistry, 281(13), 8917–8926. 10.1074/jbc.M509344200 [PubMed: 16418172]

Fujita Y, Komatsu N, Matsuda M, & Aoki K. (2014). Fluorescence resonance energy transfer based quantitative analysis of feedforward and feedback loops in epidermal growth factor receptor signaling and the sensitivity to molecular targeting drugs. FEBS Journal, 281(14), 3177–3192. 10.1111/febs.12852 [PubMed: 24848561]

Germond A, Fujita H, Ichimura T, & Watanabe TM (2016). Design and development of genetically encoded fluorescent sensors to monitor intracellular chemical and physical parameters. Biophysical Reviews, 8(2), 121–138. 10.1007/s12551-016-0195-9 [PubMed: 28510054]

Gillies TE, Pargett M, Silva JM, Teragawa CK, McCormick F, & Albeck JG (2020). Oncogenic mutant RAS signaling activity is rescaled by the ERK/MAPK pathway. Molecular Systems Biology, 16(10), 1–19. 10.15252/msb.20209518

Gonze D, Gérard C, Wacquier B, Woller A, Tosenberger A, Goldbeter A, & Dupont G. (2018). Modeling-based investigation of the effect of noise in cellular systems. Frontiers in Molecular Biosciences, 5( ), 1–12. 10.3389/fmolb.2018.00034 [PubMed: 29417049]

Greenwald EC, Mehta S, & Zhang J. (2018). Genetically encoded fluorescent biosensors illuminate the spatiotemporal regulation of signaling networks. Chemical Reviews, 118(24), 11707–11794. 10.1021/acs.chemrev.8b00333 [PubMed: 30550275]

Greenwald E, Polanowska-Grabowska R, & Saucerman J. (2014). Integrating Fluorescent Biosensor Data Using Computational Models. Methods in molecular biology (Clifton, N.J.), 1071, 227–248. 10.1007/978-1-62703-622-1_18

Greenwald E, Posner C, Bharath A, Lyons A, Salmerón C, Sriram K, et al. (2023). GPCR Signaling Measurement and Drug Profiling with an Automated Live-Cell Microscopy System. ACS Sensors, 8(1), 19–27. 10.1021/acssensors.2c01341 [PubMed: 36602887]

Hinke SA, Navedo MF, Ulman A, Whiting JL, Nygren PJ, Tian G, et al. (2012). Anchored phosphatases modulate glucose homeostasis. The EMBO Journal, 31(20), 3991–4004. 10.1038/emboj.2012.244 [PubMed: 22940692]

Irannejad R, Tomshine JC, Tomshine JR, Chevalier M, Mahoney JP, Steyaert J, et al. (2013). Conformational biosensors reveal GPCR signalling from endosomes. Nature, 495(7442), 534–538. 10.1038/nature12000 [PubMed: 23515162]

Kudo T, Jeknić S, Macklin DN, Akhter S, Hughey JJ, Regot S, & Covert MW (2018). Live-cell measurements of kinase activity in single cells using translocation reporters. Nature Protocols, 13(1), 155–169. 10.1038/nprot.2017.128 [PubMed: 29266096]

Lai HT, Griesbeck O, & Yue DT (2007). Live-cell transforms between Ca^{2+} transients and FRET responses for a troponin-C-based Ca^{2+} sensor. Biophysical Journal, 93(11), 4031–4040. 10.1529/biophysj.107.109629 [PubMed: 17704158]

Lohse C, Bock A, Maiellaro I, Hannawacker A, Schad LR, Lohse MJ, & Bauer WR (2017). Experimental and mathematical analysis of cAMP nanodomains. PLoS ONE, 12(4), 1–19. 10.1371/journal.pone.0174856

MacDonald PE, & Rorsman P. (2006). Oscillations, intercellular coupling, and insulin secretion in pancreatic β cells. PLoS Biology, 4(2), 167–171. 10.1371/journal.pbio.0040049

Mehta S, & Zhang J. (2021). Biochemical Activity Architectures Visualized-Using Genetically Encoded Fluorescent Biosensors to Map the Spatial Boundaries of Signaling Compartments. Accounts of Chemical Research, 54(10), 2409–2420. 10.1021/acs.accounts.1c00056 [PubMed: 33949851]

Mehta S, Zhang Y, Roth RH, Zhang J.fan, Mo A, Tenner B., et al. (2018). Single-fluorophore biosensors for sensitive and multiplexed detection of signalling activities. Nature Cell Biology, 20(10), 1215–1225. 10.1038/s41556-018-0200-6 [PubMed: 30250062]

Mo GCH, Ross B, Hertel F, Manna P, Yang X, Greenwald EE, et al. (2017). Genetically encoded biosensors for visualizing live-cell biochemical activity at super-resolution. Nat Methods, 14(4), 427–434. 10.1038/nMeth.4221 [PubMed: 28288122]

Murphy JG, Sanderson JL, Gorski JA, Scott JD, Catterall WA, Sather WA, & Dell'Acqua ML (2014). AKAP-anchored PKA maintains neuronal L-type calcium channel activity and NFAT transcriptional signaling. Cell Reports, 7(5), 1577–1588. 10.1016/j.celrep.2014.04.027 [PubMed: 24835999]

Nasu Y, Shen Y, Kramer L, & Campbell RE (2021). Structure- and mechanism-guided design of single fluorescent protein-based biosensors. Nature Chemical Biology, 17(5), 509–518. 10.1038/s41589-020-00718-x [PubMed: 33558715]

Ni Q, Ganesan A, Aye-Han NN, Gao X, Allen MD, Levchenko A, & Zhang J. (2011). Signaling diversity of PKA achieved via a Ca^{2+} -cAMP-PKA oscillatory circuit. Nature Chemical Biology, 7(1), 34–40. 10.1038/nchembio.478 [PubMed: 21102470]

Palmer AE, Qin Y, Park JG, & McCombs JE (2011). Design and application of genetically encoded biosensors. Trends in Biotechnology, 29(3), 144–152. 10.1016/j.tibtech.2010.12.004 [PubMed: 21251723]

Regot S, Hughey JJ, Bajar BT, Carrasco S, & Covert MW (2014). High-sensitivity measurements of multiple kinase activities in live single cells. Cell, 157(7), 1724–1734. 10.1016/j.cell.2014.04.039 [PubMed: 24949979]

Ryu H, Chung M, Dobrzyński M, Fey D, Blum Y, Lee SS, et al. (2015). Frequency modulation of ERK activation dynamics rewires cell fate. Molecular Systems Biology, 11(11), 838. 10.15252/msb.20156458 [PubMed: 26613961]

Sachs K, Gifford D, Jaakkola T, Sorger P, & Lauffenburger DA (2002). Bayesian network approach to cell signaling pathway modeling. Science's STKE : signal transduction knowledge environment, 2002(148), 1–6. 10.1126/stke.2002.148.pe38

Sachs K, Perez O, Pe'er D, Lauffenburger DA, & Nolan GP (2005). Causal protein-signaling networks derived from multiparameter single-cell data. Science, 308(5721), 523–529. 10.1126/science.1105809 [PubMed: 15845847]

Seino S, & Shibasaki T. (2005). PKA-dependent and PKA-independent pathways for cAMP-regulated exocytosis. Physiological Reviews, 85(4), 1303–1342. 10.1152/physrev.00001.2005 [PubMed: 16183914]

Soheilypour M, & Mofrad MRK (2018). Agent-Based Modeling in Molecular Systems Biology. BioEssays, 40(7), 1–8. 10.1002/bies.201800020

Székely T, & Burrage K. (2014). Stochastic simulation in systems biology. Computational and Structural Biotechnology Journal, 12(20–21), 14–25. 10.1016/j.csbj.2014.10.003 [PubMed: 25505503]

Takano T, Wu M, Nakamuta S, Naoki H, Ishizawa N, Namba T, et al. (2017). Discovery of long-range inhibitory signaling to ensure single axon formation. Nature Communications, 8(1), 1–17. 10.1038/s41467-017-00044-2

Tenner B, Getz M, Ross B, Ohadi D, Bohrer CH, Greenwald E, et al. (2020). Spatially compartmentalized phase regulation of a Ca^{2+}-cAMP-PKA oscillatory circuit. eLife, 9, 1–34. 10.7554/eLife.55013

Tyson JJ, Laomettachit T, & Kraikivski P. (2019). Modeling the dynamic behavior of biochemical regulatory networks. Journal of Theoretical Biology, 462, 514–527. 10.1016/j.jtbi.2018.11.034 [PubMed: 30502409]

Várnai P, Rother KI, & Balla T. (1999). Phosphatidylinositol 3-Kinase-dependent Membrane Association of the Bruton's Tyrosine Kinase Pleckstrin Homology Domain Visualized in Single Living Cells *. Journal of Biological Chemistry, 274(16), 10983–10989. 10.1074/jbc.274.16.10983

Willoughby D, Halls ML, Everett KL, Ciruela A, Skroblin P, Klussmann E, & Cooper DMF (2012). A key phosphorylation site in AC8 mediates regulation of Ca^{2+}-dependent cAMP dynamics by an AC8–AKAP79–PKA signalling complex. Journal of Cell Science, 125(23), 5850–5859. 10.1242/jcs.111427 [PubMed: 22976297]

Yang JH, Polanowska-Grabowska RK, Smith JS, Shields CW, & Saucerman JJ (2014). PKA catalytic subunit compartmentation regulates contractile and hypertrophic responses to β-adrenergic signaling. Journal of Molecular and Cellular Cardiology, 66, 83–93. 10.1016/j.yjmcc.2013.11.001 [PubMed: 24225179]

Yang JH, & Saucerman JJ (2011). Computational models reduce complexity and accelerate insight into cardiac signaling networks. Circulation Research, 108(1), 85–97. 10.1161/CIRCRESAHA.110.223602 [PubMed: 21212391]

Yang JM, Chi WY, Liang J, Takayanagi S, Iglesias PA, & Huang CH (2021). Deciphering cell signaling networks with massively multiplexed biosensor barcoding. Cell, 184(25), 6193–6206.e14. 10.1016/j.cell.2021.11.005

Zhang JF, Mehta S, & Zhang J. (2021). Signaling Microdomains in the Spotlight: Visualizing Compartmentalized Signaling Using Genetically Encoded Fluorescent Biosensors. Annual Review of Pharmacology and Toxicology, 61, 587–608. 10.1146/annurev-pharmtox-010617-053137

Zhang JZ, Lu TW, Stolerman LM, Tenner B, Yang JR, Zhang JF, et al. (2020). Phase Separation of a PKA Regulatory Subunit Controls cAMP Compartmentation and Oncogenic Signaling. Cell, 182(6), 1531–1544.e15. 10.1016/j.cell.2020.07.043

Zhang JZ, Nguyen AH, Miyamoto S, Brown JH, McCulloch AD, & Zhang J. (2020). Histamine-induced biphasic activation of RhoA allows for persistent RhoA signaling. PLoS Biology, 18(9), 1–23. 10.1371/journal.pbio.3000866

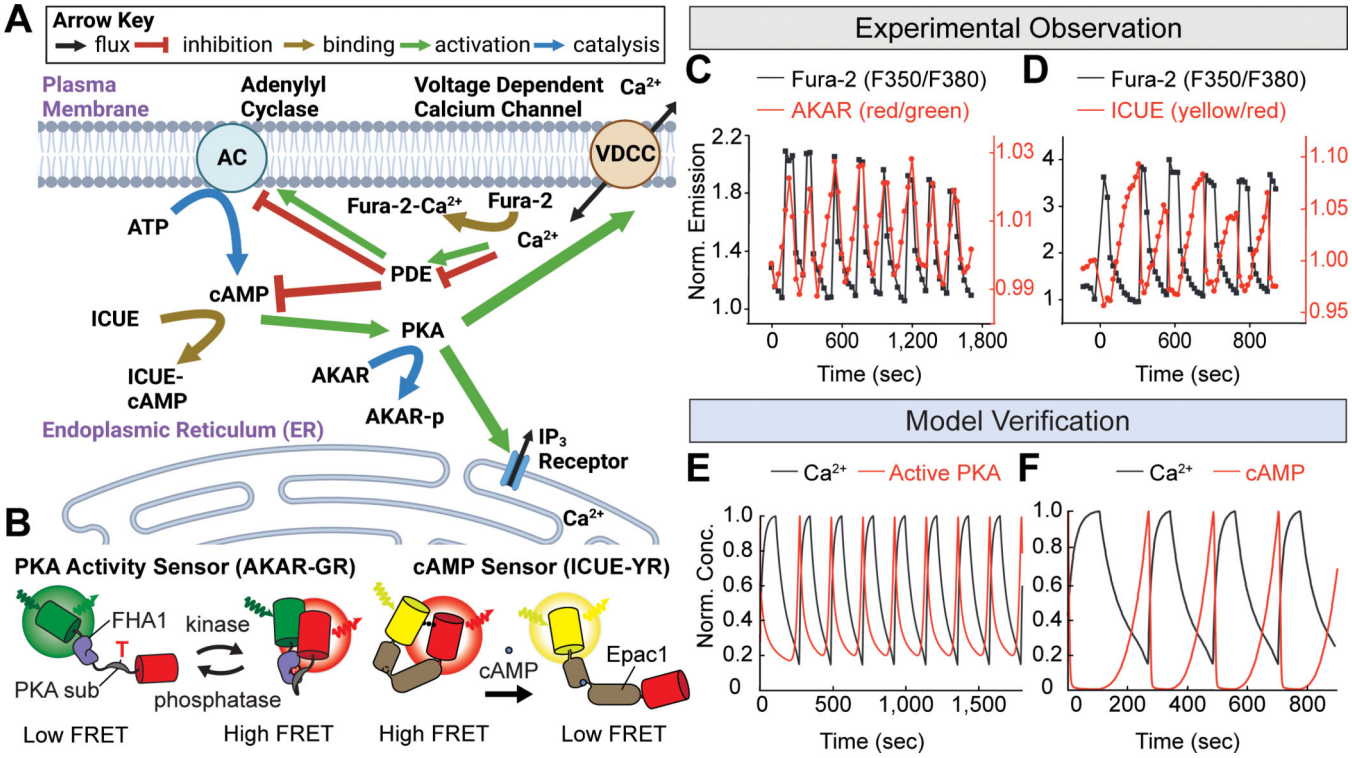

Figure 1. Interplay between cAMP, PKA, and Ca^{2+} in β cells.

A) Key components in the computational model of the cAMP, PKA, and Ca^{2+} circuit. PKA can modulate Ca^{2+} flux into the cytosol from extracellular or intracellular sources by phosphorylating and activating Voltage Dependent Calcium Channels and IP_3 receptors, respectively. Calcium can modulate cAMP by activating or inhibiting adenylyl cyclase or phosphodiesterases (PDEs), which produce and degrade cAMP, respectively. B) Schematics of the PKA Activity biosensor (AKAR-GR) and cAMP biosensor (ICUE-YR) used in co-imaging experiments. When PKA phosphorylates the PKA substrate sequence on AKAR-GR, FHA1 will bind to the phosphorylated residue, causing a conformational change in the sensor that increases FRET. cAMP binds to Epac-1 region of ICUE-YR, causing a conformational change in the sensor that decreases FRET. C & D) Multiplexing experimental results with Fura-2 and AKAR-GR (C) or Fura-2 and ICUE-YR (D). Co-imaging Fura-2 and AKAR-GR shows in-phase PKA-Ca^{2+} oscillations (C). Co-imaging Fura-2 and ICUE-YR reveals out-of-phase cAMP-Ca^{2+} oscillations (D). E & F) To investigate the cAMP, PKA, and Ca^{2+} circuit, we built a minimal ordinary differential equation (ODE) model to qualitatively match the experimental results observed in C and D. The model qualitatively recapitulates in-phase PKA-Ca^{2+} oscillations (E) and out-of-phase cAMP-Ca^{2+} oscillations (F). Panel A was made using Biorender.com. Panels C-F were taken from figures in Ni et al. 2011.

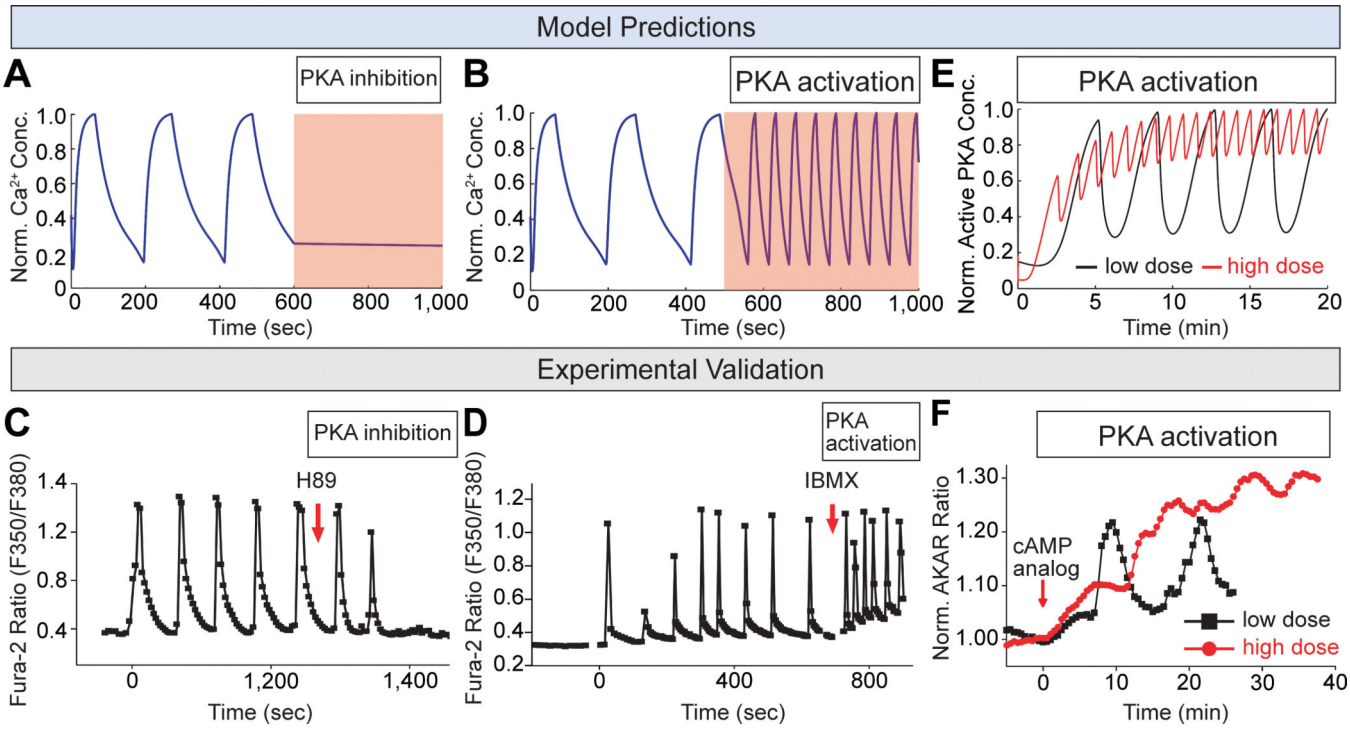

Figure 2. PKA Tunes Ca^{2+} Oscillations, and PKA Activity Oscillates upon Direct Activation.

A) The model predicts that inhibiting PKA activity (shaded region) will abrogate Ca^{2+} oscillations. B) The model predicts that increasing PKA activity (shaded region) will tune the frequency of Ca^{2+} oscillations. C) Fura-2 calcium imaging with PKA inhibition by 10 μM H89, an ATP-competitive PKA inhibitor, confirms that PKA inhibition blocks Ca^{2+} oscillations. D) Fura-2 calcium imaging with indirect PKA activation by 100 μM IBMX, a phosphodiesterase inhibitor, confirms that PKA activation increases the frequency of Ca^{2+} oscillations. E) The model predicts that activating PKA activity with a low dose of activator yields lower frequency oscillations in PKA activation while a high dose induces higher frequency oscillations in PKA activation. F) FRET imaging of the AKAR biosensor confirms a low dose (1–3 μM) of 8-bromoadenosine-3′, 5′-cyclic monophosphate acetoxymethylester, a PKA-specific cAMP analog, yields lower-frequency oscillations in PKA activity while a high dose (10–20 μM) induces higher-frequency oscillations in PKA activity. This figure was created using figures in Ni et al. 2011.

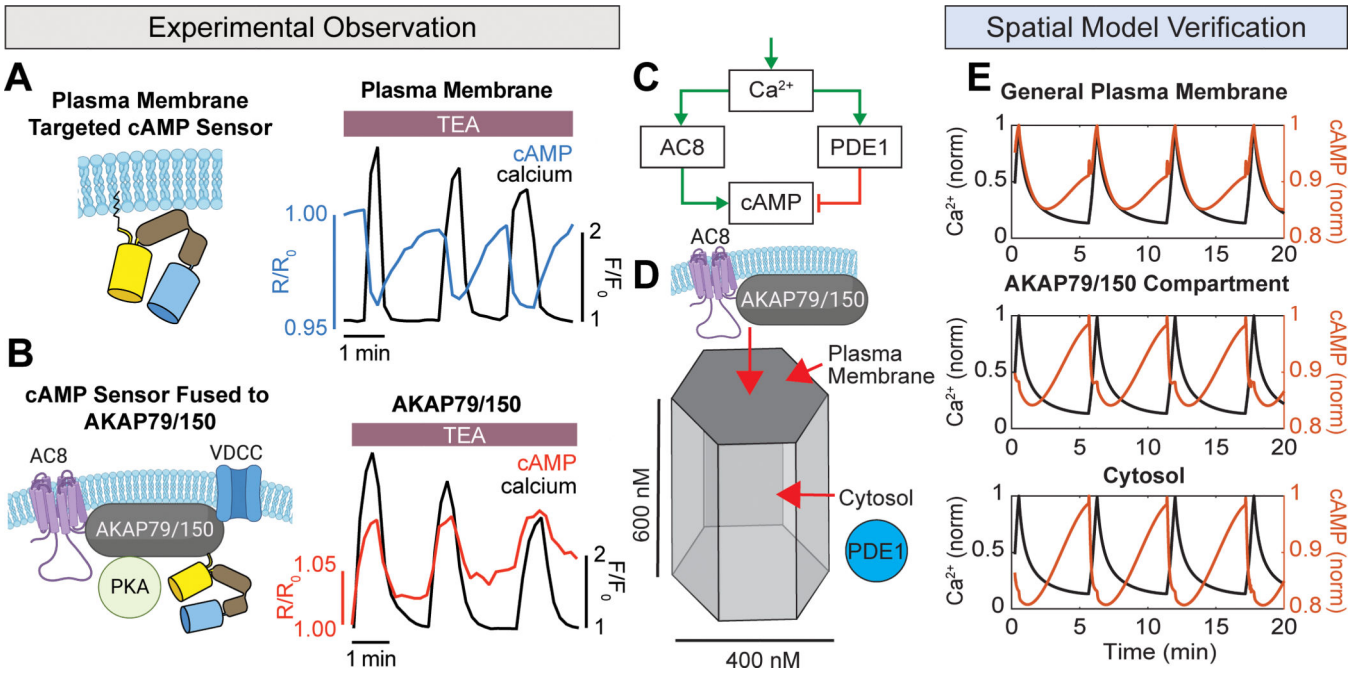

Fig 3. Biosensor Targeting and Spatial Modeling Reveals Distinct Tuning of the Ca^{2+}-cAMP-PKA Oscillatory Circuit within AKAP79/150 Compartment.

A) Schematic of the cAMP biosensor targeted to the plasma membrane and the experimental results showing out-of-phase oscillations between cAMP and Ca^{2+} at the plasma membrane. Oscillations were induced by the application of tetraethylammonium (TEA), which depolarizes the plasma membrane to trigger Ca^{2+} influx. B) Schematic of the cAMP biosensor tethered to AKAP79/150 for measuring cAMP levels at the AKAP79/150 compartment and experimental results showing in-phase oscillations between cAMP and Ca^{2+} at the AKAP79/150 compartment. C) The simplified model network of cAMP, Ca^{2+}, and Ca^{2+}-activated AC8 and PDE1, which produce and degrade cAMP, respectively. D) Spatial model dimensions and shape. The center of the top face of the hexagonal prism contains one immobile AKAP79/150:AC8 cluster, and the cytosol contains a uniform concentration of PDE1. E) Model predicted oscillations in phase at center of the AKAP79/150 compartment and out of phase outside of the compartment at the general plasma membrane or in the cytosol, matching experimental data obtained using biosensors. This figure was made in part using Biorender.com. Graphs in Panels A, B, and E were created from figures in Tenner et al. 2020 and is licensed by CC BY.

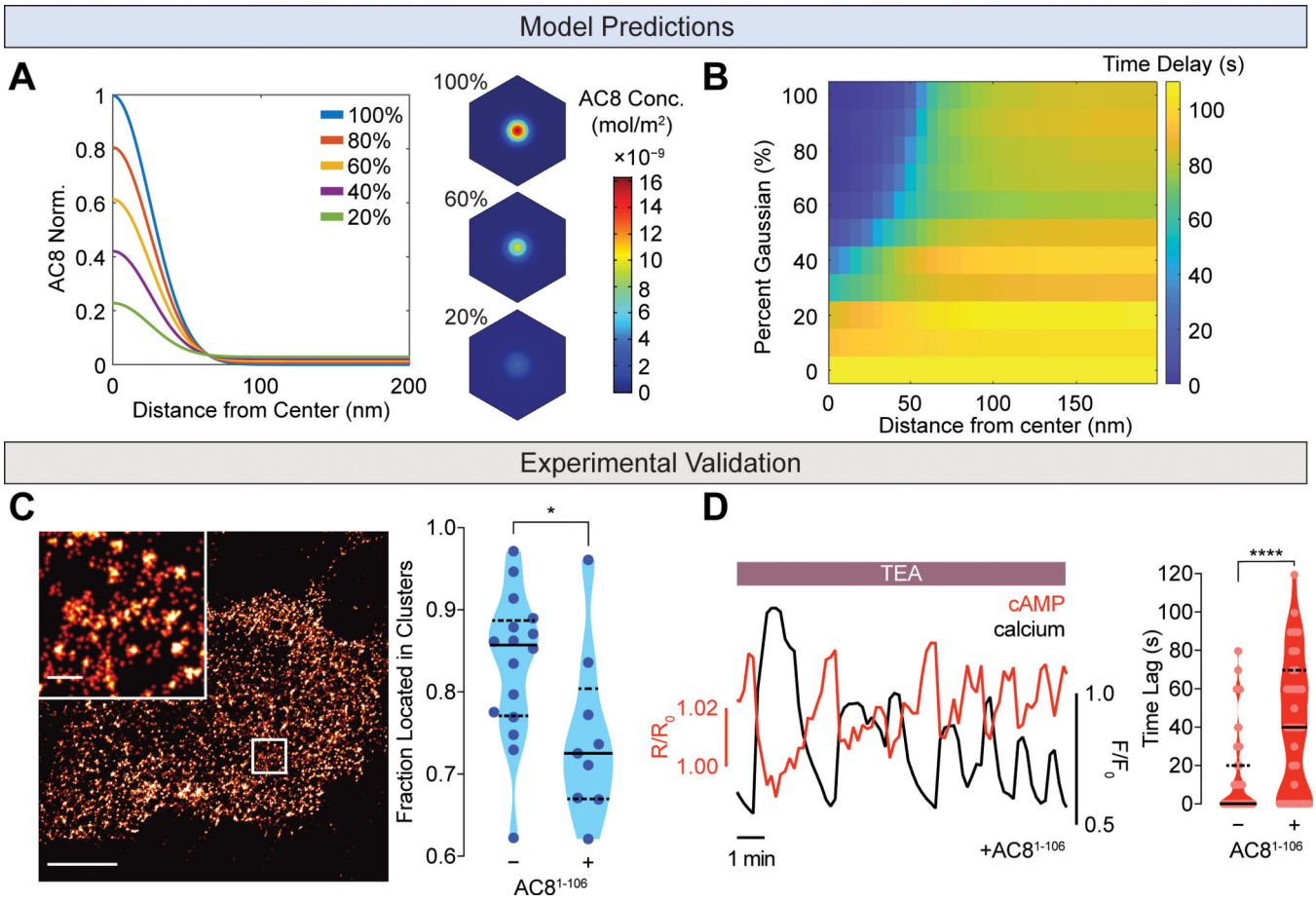

Figure 4. AKAP79/150:AC8 Interaction Strength Important in AC8 Localization and cAMP-Ca^{2+} Oscillation Phase Relationship.

A) Spatial model prediction that the disruption of the AKAP79/150:AC8 interaction causes redistribution of AC8 from within the cluster to the plasma membrane (measured as percent Gaussian) shown as half-Gaussian cross-sections in graph on the left and representative AC8 concentration heat maps of the hexagonal plasma membrane surface of 3D model on the right. B) Heatmap of the spatial model prediction that decreasing AC8 localization within the cluster or increasing distance from the cluster increases the time lag between cAMP and Ca^{2+} oscillations. C) Representative super-resolution image (scale 5 μM, inset 500 nm) of over-expression of $AC8^{1-106}$, which disrupts AKAP79/150:AC8 clustering by competitively interacting with AKAP79/150, and quantification of decrease in the percent of AC8 localizations that fall into AKAP nanoclusters with $AC8^{1-106}$ overexpression compared to wild type. D) In agreement with model predictions, the disruption of AKAP79/150:AC8 interaction by overexpression of $AC8^{1-106}$ leads to an increase in time lag between cAMP and Ca^{2+} oscillations at the AKAP79/150 compartment as measured using FRET biosensor imaging. This figure was created from figures in Tenner et al. 2020 and is licensed by CC BY.

Table 1.

Summary of Example Computational Models Combined with Biosensor Data

Modeling Question	Biosensor	Model	Study Findings	Reference
What causes biphasic RhoA response to histamine stimulation in HeLa cells?	FRET-based RhoA activation biosensor (DORA RhoA)	ODE model of RhoA signaling with two divergent upstream pathways	• First phase of RhoA response depends on p63 RhoGEF and continuously active histamine receptor • Second phase of RhoA response depends on p115 RhoGEF, insensitive to rapid turning off of the receptor	J. Z. Zhang, Nguyen, et al. 2020
What causes heterogenous ERK kinetics in response to sustained growth factor stimulation versus homogenous ERK transients in response to pulsed growth factor simulation in PC-12 cells?	FRET-based ERK activity biosensor (EKAR2G)	Semi-deterministic ODE model with activated receptor and Ras GTPase activation of Raf/MEK/ERK signaling cascade	• A receptor activity dependent, feed-forward mechanism from ERK onto the upstream Raf kinase causes heterogeneous ERK kinetics in response to sustained stimulation. • This feed-forward mechanism is bypassed during pulsed stimulation.	Ryu et al. 2015
What causes differences in PKA sensitivity and kinetics to β-adrenergic receptor agonist isoproterenol in the nucleus versus the cytosol in cardiomyocytes?	FRET-based PKA activity biosensor (AKAR)	ODE model of PKA signaling with 3 subcellular compartments: plasma membrane, cytosol, and nucleus	• PKA activity in the nucleus is rate-limited by slow diffusion of PKA catalytic subunit. • Lower sensitivity of nuclear PKA due to nuclear expression of protein kinase inhibitor (PKI)	J. H. Yang et al. 2014
What causes greater maximal cAMP response at lipid-raft regions than non-raft regions of the plasma membrane in neonatal rat ventricular myocytes?	FRET-based cAMP reporter (Epac2-camps)	ODE model of cAMP signaling with 3 domains: lipid raft domains of plasma membrane, non lipid-raft domains of the plasma membrane, and bulk cytosol domain	• Differences in maximal cAMP responses due to higher basal cAMP concentrations in non-raft plasma membrane regions • Limited diffusion of cAMP between lipid-raft and non-raft domains is required for cAMP compartmentation between the two domains.	Agarwal et al. 2014
Is phosphodiesterase activity alone sufficient to create experimentally observed cAMP sinks around phosphodiesterases in HEK293-TsA cells?	FRET-based cAMP reporter fused to phosphodiesterase PDE4A1 (Epac1-camps-PDE4A1)	PDE model of cAMP diffusion and degradation around a spherical phosphodiesterase or cluster of spherical phosphodiesterases	• Phosphodiesterase activity alone cannot explain cAMP nano-compartments, which require additional factors such as restricted diffusion of cAMP to form.	Lohse et al. 2017
Does RhoA and Rho-kinase control the formation of a single axon from many minor neurites in polarized neurons?	FRET-based RhoA activation sensor (Raichu-RhoA) and photoactivatable RhoA (LOVTRAP- RhoA) and Rho-kinase (LOVTRAP-Rho-kinase)	PDE model of Rho-kinase diffusion along minor and major neurites	• Rho-kinase accumulates more in minor neurites compared to the long neurite, which retracts the growing minor neurites to ensure that only one axon forms.	Takano et al. 2017